

# Research on the influence of performance parameters on the super high speed permanent magnet synchronous generator external characteristic

HONGBO QIU, BINQIA TANG, CUNXIANG YANG, GUANGZHAO CUI

*College of Electric and Information Engineering  
Zhengzhou University of Light Industry  
Zhengzhou 450002, China  
e-mail: yangcx77777@163.com*

(Received: 17.05.2017, revised: 12.01.2018)

**Abstract:** Super high speed permanent magnet generators (SHSPMG) usually operate at high frequency. The external characteristic of the SHSPMG under condition of high frequency operation is quite different from that of conventional generators. Therefore, it is necessary to study the external characteristic of the SHSPMG. Based on the finite element method, this paper studied the factors that affect the external characteristic of the SHSPMG. Combining the vector method and the finite element method, the external characteristic of the SHSPMG with the inductive load and the resistance load was studied. The variation law of the generator terminal voltage with the change of the load and current was obtained, and the key factors affecting the external characteristic of the SHSPMG were determined. The influences of the armature resistance, power factor, frequency and permanent magnet performance on the external characteristic of the SHSPMG were studied. The influence mechanism of different parameters on the generator external characteristic was revealed. The influence degree of each factor on the voltage regulation was determined. The conclusions can provide reference for the design and research of the SHSPMG.

**Key words:** external characteristic, influence degree, performance parameters, super high speed permanent magnet generator

## 1. Introduction

The super high speed permanent magnet synchronous generator has advantages of high power density, high power generation efficiency [1–4], no need of a collector ring and brush device and so on, and it can be connected with the driving device directly, so the SHSPMG is used widely in a distributed generation system. The power generated by the SHSPMG is high-frequency, which could not be used by users directly. Therefore, the power should be converted into direct current through AC/DC converters and then be converted to alternating current through DC/AC

converters. After the conversion, it could be used. However, in the conversion process, due to the change of the controller control strategy, the output current and voltage will change. When loads change, the generator performance will also change. At the same time, the voltage regulation of permanent magnet generators is difficult [5]. The study on the generator external characteristic is conducive to analyzing the voltage fluctuation caused by the load change during the generator operation, and it is of great significance to master the running state and ensure the stable and normal operation of generators.

In recent years, many researches have been carried out on the relationship between the current and voltage of generators. In reference [6], the magnetic field of a high speed electrical excitation flux-switching (EEFS) machine was analyzed and the structure was optimized. The no-load operation performance including the external characteristic was analyzed. In reference [7], a novel integrated brushless excitation method for a rotor-excited generator was proposed, and the no-load, external regulation and excitation characteristics were analyzed. In reference [8], a novel hybrid rotor structure of a brushless doubly fed machine was designed, and the no-load characteristic is significantly greater compared with the traditional rotor structure. In reference [9], a novel brushless coordinate structure hybrid excitation synchronous generator (HESG) with AC excitation was proposed and the no-load characteristic, external behaviors and the regulation characteristic were simulated. However, there are few studies on the external characteristic aiming at the SHSPMG.

External characteristic is an important performance index of the SHSPMG, which determines the generator stability. In order to pursue better generator performance and stable generator operation, it is necessary to research the external characteristic of the SHSPMG. Therefore, the change law of the external characteristic and the main factors affecting the external characteristic are analyzed in this paper. Combining the vector method and the finite element method, the external characteristic of the SHSPMG with different loads is studied. The variation of the generator terminal voltage with the load and current change is obtained, and the key factors affecting the external characteristic of the SHSPMG are determined. Based on the influence of each performance parameter on the generator external characteristic, the influence mechanism of each factor on the generator external characteristic is analyzed and determined. The conclusions could provide some useful reference for the design and research of the SHSPMG.

## 2. Model establishment and experimental verification

### 2.1. Generator model and basic parameters

In this paper, an 117 kW and 60 000 rpm SHSPMG is taken as an example, and based on the actual generator structure, a two-dimensional finite element model is established, as shown in Fig. 1.

The material of the sleeve is the high strength austenitic steel (50Mn18Cr5). The alloy sleeve (50Mn18Cr5) contains C by 0.5%, Mn by 18%, Cr by 5%, Si by 0.5%, and so on. The relative permeability is 1, and the bulk conductivity is  $1.31 \times 10^6$  S/m. The material of the core is the silicon steel sheet DW310-35. The hysteresis loss coefficient  $K_h$  equals 305.82, the classical eddy current loss coefficient  $k_c$  equals 0.30, and the additional eddy current loss coefficient  $k_e$  equals 0.64. The stator windings of the SHSPMG adopt back round structure, whose purpose is to reduce

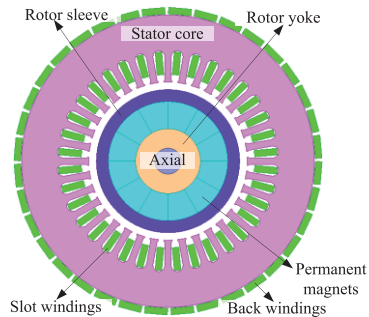


Fig. 1. The finite element model

the axial length of the rotor. One side of the winding coil is embedded in the stator iron core slot, and the other side is placed in the middle of the yoke back of the stator core. Eight permanent magnets are attached to the rotor surface. Permanent magnets are segmented in axial direction in order to reduce the eddy current loss [10]. In order to prevent permanent magnets from falling off during high speed rotation, a sleeve is needed on the surface of permanent magnets. The flux line distribution of the generator under no-load condition at rated speed is shown in Fig. 2.

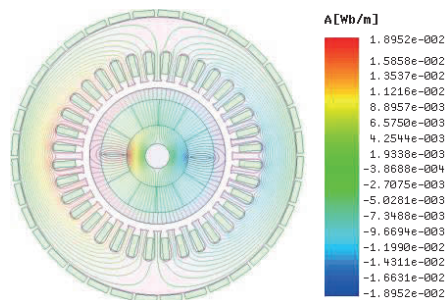


Fig. 2. Distribution of the flux lines under no load condition

It could be seen from the distribution of the flux lines that there is one pair of magnetic pole, which is consistent with the actual generator. Closed flux line loop is shaped in the magnetization direction of the generator, through the permanent magnets, sleeve, air gap, stator teeth and stator yoke.

The stator end of the SHSPMG and the prototype are shown as Fig. 3. The basic parameters are shown in Table 1. In order to simplify the calculation, the following assumptions are made in the electromagnetic analysis of the SHSPMG [11–12]:

1. The electromagnetic field of the generator varies less due to the slender core. Therefore, the magnetic vector potential only has the component in  $z$ -direction in the analysis of the two-dimensional transient field. At the same time, the magnetic flux leakage of the generator is neglected.
2. Materials are isotropic. The permeability of the materials is uniform and the variation of the permeability with the temperature is ignored.
3. Displacement current is ignored.

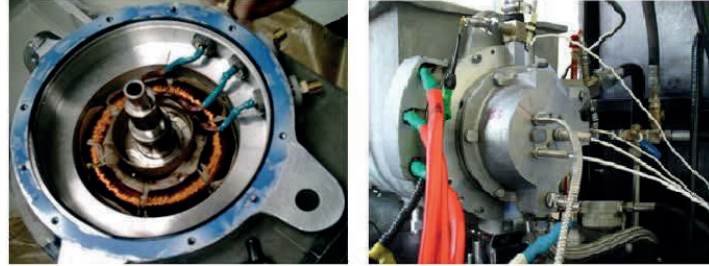


Fig. 3. Prototype and stator end of the SHSPMG

4. The end effect considered in this paper includes the end winding resistance and the end winding leakage inductance, which are employed in the field-circuit coupling calculation, just as shown in Fig. 4.

The transient two-dimensional electromagnetic field calculation equation is as follows [13]:

$$\left\{ \begin{array}{l} \Omega: \frac{\partial}{\partial x} \left( \frac{1}{\mu} \frac{\partial A_z}{\partial x} \right) + \frac{\partial}{\partial y} \left( \frac{1}{\mu} \frac{\partial A_z}{\partial y} \right) = - \left( J_z - \sigma \frac{dA_z}{dt} \right) \\ \Gamma_1: A_z = 0 \\ \Gamma_2: \frac{1}{\mu_1} \frac{\partial A_z}{\partial n} - \frac{1}{\mu_2} \frac{\partial A_z}{\partial n} = J_s \end{array} \right. , \quad (1)$$

where:  $\Omega$  is the calculation region;  $A_z$  and  $J_z$  are the magnetic vector potential and the source current density in the  $z$ -axial component, respectively;  $J_s$  is the equivalent face current density of permanent magnets;  $\sigma$  is the conductivity;  $\Gamma_1$  is the parallel boundary condition;  $\Gamma_2$  is the permanent magnet boundary condition; and  $\mu_1$  and  $\mu_2$  are relative permeability values.

Table 1. Basic parameters of the SHSPMG prototype

Basic parameters	Value	Basic parameters	Value
Rated power (kW)	117	Stator outer diameter (mm)	135
Rated voltage (V)	670	Stator inner diameter (mm)	72
Pole number	2	Rotor outer diameter (mm)	66
Rotor type	PM	Core length (mm)	275
Frequency (Hz)	1 000	Slot number	36
Parallel branch number	1	Thickness of permanent magnets (mm)	12.5
Winding connection type	Y	Thickness of sleeve (mm)	2

In this paper, the field-circuit coupling method is adopted to analyze the electromagnetic field of the SHSPMG. The external circuit is shown in Fig. 4.

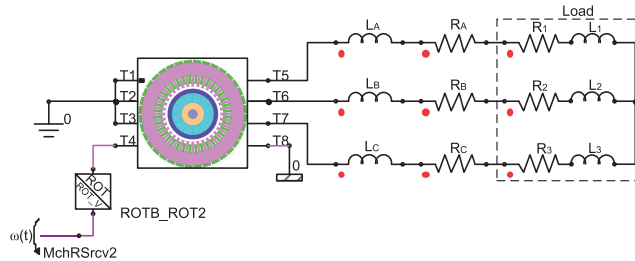


Fig. 4. External circuit of the SHSPMG

where:  $L_A$ ,  $L_B$ , and  $L_C$  are the end leakage inductances,  $R_A$ ,  $R_B$ , and  $R_C$  are the winding resistances,  $L_1$ ,  $L_2$ , and  $L_3$  are the load inductances and  $R_1$ ,  $R_2$ , and  $R_3$  are the load resistances.

### 2.2. Experimental test and data comparison

In order to verify the correctness of the finite element model, the SHSPMG prototype was tested. Experimental equipment such as the power quality analyzer, the power analyzer and the high speed torque and rotational speed sensor device was used. The test platform is shown in Fig. 5. By experiment, the terminal voltage and the armature current of the generator running at a speed of 6 000 rpm, 8 000 rpm and 10 000 rpm were obtained respectively. The experimental data are compared with the finite element model calculated results, as shown in Table 2.

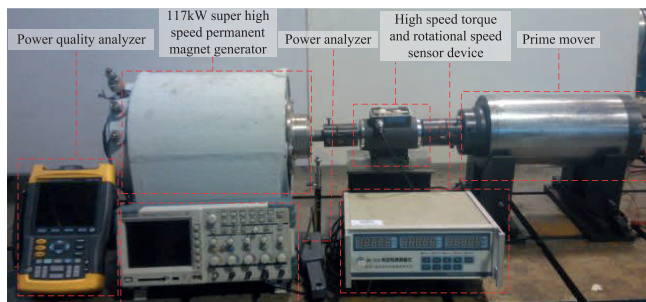


Fig. 5. The test platform

Table 2. Comparison of the test data and the finite element model calculated results

Speed (rpm)		6 000	8 000	10 000
Calculated results	Terminal voltage (V)	39.9	53.1	65.8
	Armature current (A)	14.5	18.3	22.4
Test data	Terminal voltage (V)	39.6	53.7	65.1
	Armature current (A)	14.4	18.5	22.1

It could be seen from the data in Table 2 that the experimental data are in good agreement with the model calculated results, which verifies the accuracy of the finite element model.

### 3. Analysis of influence factors of the inherent voltage regulation rate (IVRR)

The external characteristic is one of the most important characteristics of the SHSPMG. Many factors affect the external characteristic. In order to get better generator performance, it is necessary to analyze the influence factors on the external characteristic of the SHSPMG.

The IVRR of the generator is usually used as a performance index to measure the external characteristic. IVRR is one of the most important performance indexes of the SHSPMG, and the numerical value of the IVRR has important reference value for the generator performance. The smaller the IVRR value is, the better the stability of the output voltage is. Therefore, by calculating the IVRR of the generator, the external characteristic of the generator can be reflected effectively. However, for SHSPMG, it is difficult to control the output voltage and power factor, because the magnetic field of permanent magnets is difficult to adjust, which limits its application scope. At the same time, the SHSPMG usually operates under high frequency condition, and the requirement of the controller output voltage is more stringent than that of the lower speed generators. In order to improve the SHSPMG performance and obtain better performance index, it is necessary to study the IVRR of the SHSPMG. Many factors can affect the IVRR, and the influence degree of each factor is different. Therefore, it is of great significance to study and analyze the factors that affect the IVRR, and it is beneficial to the operation stability and application of the generator.

The IVRR of the generator is the variation of the terminal voltage with the load change [14], shown as Formula (2)

$$\Delta u\% = \frac{E_0 - U}{U_N} \%, \quad (2)$$

where:  $U$  is the generator output voltage,  $U_N$  is the generator rated voltage,  $E_0$  is the no-load electromotive force.

The vector diagram of the SHSPMG is shown as Fig. 6.

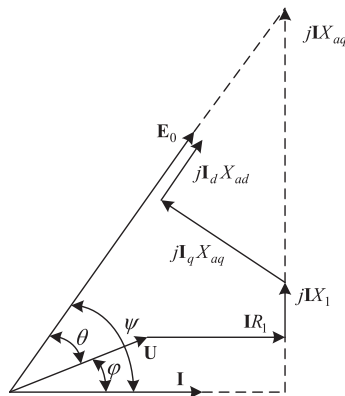


Fig. 6. The vector diagram of the SHSPMG

where:  $E_0$  is the phase electromotive force,  $U$  is the phase voltage,  $I$  is the phase current,  $R_1$  is the armature resistance of each phase,  $X_1$  is the armature winding leakage reactance,  $X_{ad}$  is the direct axis reaction armature reactance,  $X_{aq}$  is the quadrature axis reaction armature reactance,  $I_d$

is the direct axis current,  $I_q$  is the quadrature axis current,  $\theta$  is the power angle,  $\varphi$  is the external power factor angle, and  $\psi$  is the internal power factor angle.

The following relations can be obtained from the vector diagram of the permanent magnet synchronous generator.

$$(U \sin \varphi + IX_1)^2 + (U \cos \varphi + IR_1)^2 = (E_0 - I_d X_{ad})^2 + I_q^2 X_{aq}^2 \cos^2 \psi, \quad (3)$$

$$\psi = \arctan \frac{U \sin \varphi + I(X_1 + X_{aq})}{U \cos \varphi + IR_a}, \quad (4)$$

$$U = \sqrt{(E_0 - I_d X_{ad})^2 + I_q^2 X_{aq}^2 \cos^2 \psi - I^2 (R_1 \sin \varphi - X_1 \cos \varphi)^2} - I(R_1 \sin \varphi + X_1 \cos \varphi). \quad (5)$$

Lower IVRR can be achieved by increasing the output voltage. In order to increase the output voltage, on one hand, the demagnetization magnetic flux caused by the armature reaction should be reduced as much as possible, on the other hand, the armature resistance and leakage resistance voltage drop should be reduced.

Based on the above analysis and combined with the characteristics of the SHSPMG, the following factors are taken into account respectively to analyze the influence of each parameter on the external characteristic and the IVRR of the SHSPMG.

### 3.1. Influence of the armature resistance on the IVRR of the SHSPMG

The armature resistance has a significant influence on the output voltage of the SHSPMG. In order to study the IVRR of the generator with different armature resistance values, by using the finite element method, the no-load back electromotive force (EMF) and the output voltage of the generator with different values of the armature resistance are calculated. When the power factor is 0.8 and the frequency is 1 000 Hz, the IVRR with different armature resistance values is shown in Table 3.

Table 3. The IVRR with different armature resistance values

Armature resistance value ( $\Omega$ )	0.2	0.4	0.6	0.8	1
IVRR	22.26%	26.52%	30.67%	34.53%	38.51%

In Table 3, the IVRR is 22.26% when the armature resistance is 0.2  $\Omega$ . The IVRR is 30.67% when the armature resistance is 0.6  $\Omega$ . When the armature resistance increases to 1  $\Omega$ , the IVRR increases to 38.51%, which increases by 73% compared with the value when the armature resistance is 0.2  $\Omega$ . When the power factor and the frequency are constant, the IVRR increases obviously with the increase of the armature resistance. The reasons are analyzed as follows. The change of the armature resistance will have an effect on the armature reaction, which causes the air gap magnetic field distortion. When the armature resistance increases, the demagnetization caused by the armature reaction is more obvious, so the output voltage value is reduced. According to the above analysis, it can be concluded that reducing the armature resistance can reduce the IVRR of the SHSPMG effectively.

### 3.2. Influence of the frequency on the IVRR of the SHSPMG

The SHSPMG usually operates at high frequency, and the speed can even up to tens of thousands hertz per minute. In such high speed running state, the external characteristic of the SHSPMG must be different from the general speed generators. At the same time, the no-load back EMF of the generator is related to the frequency closely, and the no-load back EMF is different obviously at different speeds.

By using the finite element method, the external characteristic curves of the SHSPMG with a power factor of 0.8 and a frequency of 500 Hz and 1 000 Hz are obtained, as shown in Fig. 7.

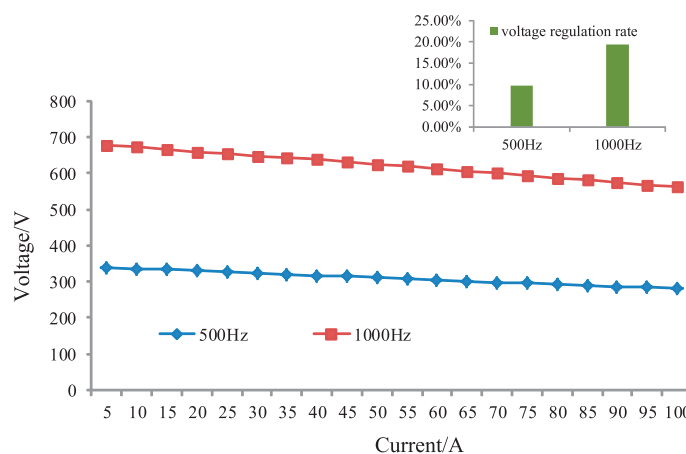


Fig. 7. External characteristic curves of the SHSPMG with a power factor of 0.8 and a frequency of 500 Hz and 1 000 Hz

In Fig. 7, the external characteristic curve of the SHSPMG with inductive load shows a downward trend. The output voltage decreases with the increase of the output current. When the output current is the same, the output voltage of the SHSPMG with 1 000 Hz is higher obviously than that with 500 Hz. Calculated by the IVRR formula, the generator IVRR is 9.63% and 19.37% when the frequency is 500 Hz and 1 000 Hz respectively. The IVRR of the SHSPMG operating at 1 000 Hz is higher obviously than that operating at 500 Hz. That is, the IVRR in high frequency operation state is higher than that in low frequency state. Therefore, under the high frequency operation, it is necessary to adopt an appropriate method to control the output voltage of the SHSPMG, in order to ensure the IVRR not too high.

Combined with the analysis of the influence of armature resistance on the voltage regulation, the IVRR with different armature resistance values is calculated when the frequency is 500 Hz and power factor is 0.8. The IVRR is shown in Table 4.

Table 4. The IVRR with different armature resistance values

Armature resistance value ( $\Omega$ )	0.2	0.4	0.6	0.8	1
IVRR	13.37%	17.39%	21.07%	24.28%	26.85%



When the frequency is 500 Hz, the IVRR also increases with the increase of the armature resistance. Combined with the data in Table 3 and Table 4, it is concluded that the IVRR when the frequency is 1 000 Hz is higher than that when the frequency is 500 Hz, as shown in Fig. 8.

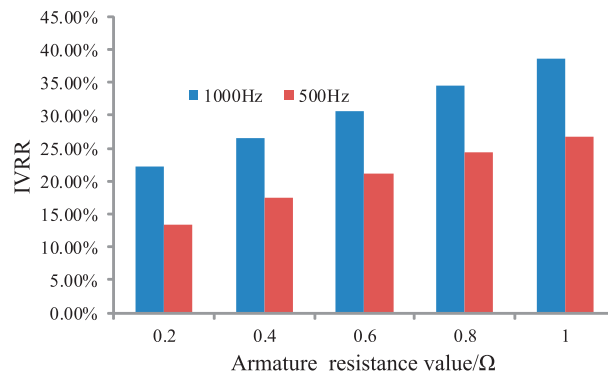


Fig. 8. The IVRR of 1 000 Hz and 500 Hz with different armature resistance values

The validity of the influence law of the armature resistance and frequency on the IVRR is verified further.

### 3.3. Influence of the power factor on the IVRR of the SHSPMG

Power factor is an important performance index of the SHSPMG. By using the finite element method, the external characteristic curves are obtained when the frequency is 1 000 Hz and the power factor is 0.8 and 1 respectively, as shown in Fig. 9.

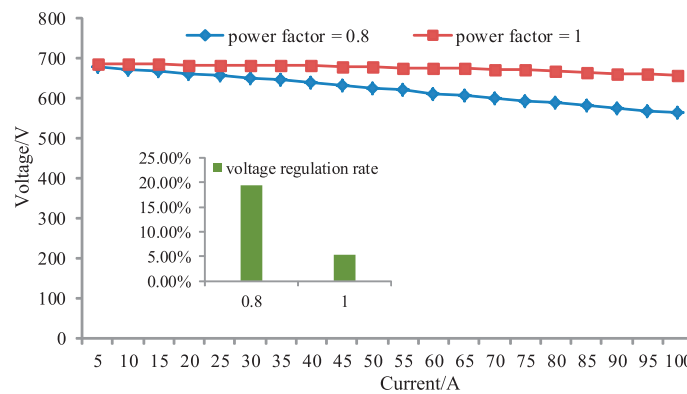


Fig. 9. External characteristic curves of the SHSPMG with the frequency of 1 000 Hz and power factor of 0.8 and 1

In Fig. 9, when the power factor is 1, the external characteristic curve of the generator is higher than that when the power factor is 0.8. When the output current is the same, the higher the power factor is, the larger the output voltage is. Accordingly, the IVRR is smaller. When the

power factor is 1, the IVRR is lower obviously than that when the power factor is 0.8. When the output current is small, the output voltage difference between the power factor of 0.8 and 1 is smaller. With the increase of the output current, the output voltage when the power factor is 1 is higher obviously than that when the power factor is 0.8. When the armature resistance and generator frequency are fixed, the increase of the power factor is conducive to reducing the IVRR of the SHSPMG. Therefore, improving the power factor of the SHSPMG has a significant effect on reducing the IVRR.

Combined with the analysis of the influence of the armature resistance and frequency on the IVRR, when the frequency is 500 Hz and 1 000 Hz respectively, the IVRR with different armature resistances is also calculated, as shown in Table 5. In Table 5, the power factor of the SHSPMG is 1.

Table 5. The IVRR when the frequency is 500 Hz and 1 000 Hz

Armature resistance ( $\Omega$ )	0.2	0.4	0.6	0.8	1
IVRR (1 000 Hz)	9.99%	15.18%	20.36%	25.54%	30.73%
IVRR (500 Hz)	7.62%	12.80%	17.98%	23.16%	28.34%

In Table 5, when the armature resistance increases, the IVRR increases. The higher the frequency is, the higher the IVRR is. The validity of the influence of armature resistance and frequency on the IVRR is further verified.

### 3.4. Influence of the permanent magnet performance on the IVRR of the SHSPMG

The magnetic field intensity generated by permanent magnets is different with different permanent magnet performance, which has a fundamental influence on the magnetic field distribution. At the same time, the demagnetization effect caused by the armature reaction of permanent magnets with different performance parameters is different. Therefore, it is necessary to study the influence of permanent magnet performance on the IVRR.

Table 6 shows the parameters of different samarium cobalt permanent magnets. The remanence and coercivity of the permanent magnet NSC811 is the largest, and the performance is the best. The permanent magnet performance of the permanent magnet NSC660 is the worst among the permanent magnets in Table 6.

Table 6. Permanent magnet performance parameters

Type of permanent magnets	NSC660	NSC700	NSC790	NSC811
$B_r$ (T)	0.87	0.92	1.04	1.07
$H_c$ (A/m)	-660 000	-700 000	-790 000	-811 000

Keeping the other conditions constant, the no-load electromotive force and the output voltage of the SHSPMG with different permanent magnet materials are calculated. The IVRR of the SHSPMG with different types of permanent magnets is calculated and analyzed. Based on the

finite element method, the IVRR of the SHSPMG is obtained when the frequency is 1 000 Hz and the power factor is 0.8. Fig. 10 shows the IVRR of the SHSPMG with different kinds of permanent magnets.

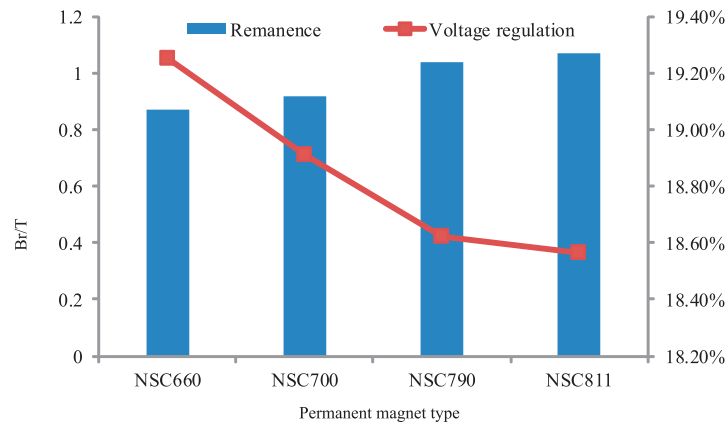


Fig. 10. The IVRR of the SHSPMG with different kinds of permanent magnets

The coercivity of the permanent magnet NSC660 is  $6.6 \times 10^5$  A/m, and the remanence is 0.87 T. When adopting the permanent magnet NSC660 whose performance is relatively poor, the IVRR of the SHSPMG is 19.25%. The coercivity of the permanent magnet NCS811 is  $8.1 \times 10^5$  A/m, and the remanence is 1.07 T. Compared with the permanent magnet NSC660, the permanent magnet NSC811 has stronger magnetism and better permanent magnet performance. When adopting the permanent magnet NSC811, the IVRR of the SHSPMG is reduced to 18.56%. The performance of permanent magnets enhances with the increase of remanence and coercivity, and with the enhancement of the permanent magnet performance, the IVRR of the SHSPMG decreases gradually.

By adopting the permanent magnet material whose coercivity is larger and the recoil permeability is smaller, the anti-demagnetization capability of permanent magnets could be improved and then the demagnetization flux caused by the armature reaction could be reduced. On the other hand, adopting the materials with larger remanence could increase the rotor leakage permeance, and then the demagnetization caused by the armature reaction could be weakened. The output voltage of the generator could be improved effectively by reducing the demagnetization effect of the armature reaction on permanent magnets. Thus, the IVRR of the SHSPMG is reduced, and the operation stability of the SHSPMG is improved.

#### 4. Analysis of the influence degree of the parameters on the external characteristic

According to the analysis of the above chapters, the IVRR could be adjusted by changing the parameters of the SHSPMG. However, the influence degree of different parameters on the external characteristic is different. Therefore, it is necessary to analyze the influence degree of

each parameter on the IVRR, in order to adjust the parameters specifically and regulate the IVRR quantitatively and effectively. In the analysis, the value of the parameter before adjustment is  $X_B$  and the value of the parameter after adjustment is  $X_A$ . The parameter adjustment rate (PAR) is defined as follow:

$$R = \frac{|X_A - X_B|}{X_B} \times 100\%. \quad (6)$$

According to the definition of the PAR, the IVRR difference of different parameters before and after adjustment with the corresponding PAR is calculated, shown as Table 7. The permanent magnet performance is measured by the remanence value.

Table 7. The IVRR difference before and after parameter adjustment

Parameters	$X_B$	$X_A$	PAR	IVRR difference before and after adjustment
Armature resistance	0.2 $\Omega$	0.4 $\Omega$	100%	4.26%
Frequency	500 Hz	1 000 Hz	100%	9.74%
Power factor	0.8	1	25%	14.08%
Permanent magnet performance	0.87 T	1.07 T	23%	0.69%

As shown in Table 7, the degree of several influence factors affecting the voltage adjustment rate is quantified. For armature resistance, when the value of the armature resistance changes from 0.2 to 0.4, the PAR is 100%, and the IVRR difference before and after adjustment is 4.26%. When the value of the frequency changes from 500 Hz to 1 000 Hz, the PAR is 100%, and the IVRR difference before and after adjustment is 9.74%. When the power factor changes from 0.8 to 1, the PAR is 25%, and the IVRR difference before and after adjustment is 14.08%. When the remanence of the permanent magnet changes from 0.87 T to 1.07 T, the PAR is 23% and the IVRR difference before and after adjustment is 0.69%.

Although the PAR of the armature resistance and the frequency is 100% and the PAR of the power factor is 25%, the variation of the IVRR caused by the adjustment of the power factor is the maximum, and the variation value before and after adjustment is 14.08%, which shows that the power factor has the greatest influence on the external characteristic with the same PAR. However, for permanent magnet performance, when the PAR is 23%, the difference between the IVRR before and after adjustment is only 0.69%. Compared with the influence of the power factor on the IVRR, the permanent magnet performance has little effect on the IVRR.

## 5. Conclusions

In this paper, the external characteristic of the SHSPMG is studied. Based on the finite element method, the influence of performance parameters on the external characteristic of the SHSPMG is researched, and the influence degree of different parameters on the external characteristic is compared and analyzed. The following conclusions are obtained:

1. With the increase of the armature resistance, the output voltage of the SHSPMG is reduced. When the power factor and the frequency are constant, the IVRR of the SHSPMG increases obviously with the increase of the armature resistance. When the armature resistance is 0.2, the IVRR is 22.26%. When the armature resistance increases to 1, the IVRR increases to 38.51%, and the IVRR increases by 73% compared with that when the armature resistance is 0.2.
2. The IVRR under low frequency operation is lower obviously than that under high frequency operation. The IVRR of 500 Hz and 1 000 Hz is 9.63% and 19.37% respectively. When the frequency increases from 500 Hz to 1 000 Hz, the IVRR is doubled.
3. The IVRR when the power factor is 1 is lower than that when the power factor is 0.8. When the power factor is 1, the IVRR is 5.29%, and when the power factor is 0.8, the IVRR is 19.37%. When the power factor is 1, the IVRR is about 3.66 times of that when the power factor is 0.8. Improving the power factor can reduce the IVRR effectively.
4. The permanent magnet performance can affect the IVRR. With the enhancement of the permanent magnet performance, the IVRR of the SHSPMG decreases gradually. The IVRR could be reduced by adopting materials with larger coercivity and remanence. When the remanence increases from 0.87 T to 1.07 T, the IVRR is reduced from 19.25% to 18.56%.
5. Through the analysis of the influence degree of different parameters on the external characteristic, it is concluded that the power factor has the greatest influence on the external characteristic, and the influence of changing the permanent magnet performance on the voltage regulation rate is not obvious compared with the power factor, frequency and armature resistance.

## References

- [1] Zhang H., Zhang X., Gerada C., Galea M., Gerada D., Li J., *Design Considerations for the Tooth Shoe Shape for High-Speed Permanent Magnet Generators*, IEEE Transactions on Magnetics, vol. 51, no. 11, pp. 1–4 (2015).
- [2] Zhang X. et al., *Electrothermal Combined Optimization on Notch in Air-Cooled High-Speed Permanent-Magnet Generator*, IEEE Transactions on Magnetics, vol. 51, no. 1, pp. 1–10 (2015).
- [3] Rahman M.A., Chiba A., Fukao T., *Super high speed electrical machines – summary*, IEEE Power Engineering Society General Meeting, Denver, CO, USA, pp. 1272–1275 (2004).
- [4] Bartolo J.B., Zhang H., Gerada D., De Lillo L., Gerada C., *High speed electrical generators, application, materials and design*, 2013 IEEE Workshop on Electrical Machines Design, Control and Diagnosis (WEMDCD), Paris, France, pp. 47–59 (2013).
- [5] Lu J., Wang D., *Research on voltage regulation range of the hybrid excitation permanent magnet generator*, 2011 International Conference on Electrical and Control Engineering, Yichang, China, pp. 803–806 (2011).
- [6] Tingting W., Meiling L., Xiaozhong Z. et al., *Magnetic field analysis and structure optimization of high speed EEFS machine*, IECON 2013 – 39th Annual Conference of the IEEE Industrial Electronics Society, Vienna, Austria, pp. 978–983 (2013).
- [7] Zhu S., Liu C., Wang K., Hu Y., Ning Y., *Theoretical and experimental analyses of a hybrid excitation synchronous generator with integrated brushless excitation*, IET Electric Power Applications, vol. 10, no. 4, pp. 258–267 (2016).

- [8] Wang X., Zhang F., Yang Q., Liu G., *Performance analysis on a novel brushless doubly fed machine with hybrid rotor structure*, 2011 International Conference on Electrical Machines and Systems, Beijing, China, pp. 1–4 (2011).
- [9] Liu M., Ji Y., Li L., Cai Z., *Research on the modeling and simulation of coordinate structure hybrid excitation synchronous generator with AC excitation*, 2011 International Conference on Electrical and Control Engineering, Yichang, China, pp. 3616–3619 (2011).
- [10] Mlot A., Łukaniszyn M., Korkosz M., *Magnet loss analysis for a high-speed PM machine with segmented PM and modified tooth-tips shape*, Archives of Electrical Engineering, vol. 65, no. 4, pp. 671–683 (2016).
- [11] Weili L., Jing W., Xiaochen Z., Baoquan K., *Loss calculation and thermal simulation analysis of high-speed PM synchronous generators with rotor topology*, 2010 International Conference on Computer Application and System Modeling (ICCASM 2010), Taiyuan, China, pp. V14-612-V14-616 (2010).
- [12] Houzhou G., Han L., Nanfan Z. et al., *3D loss and heat analysis at the end region of 4-poles 1150 MW nuclear power turbine generator*, Archives of Electrical Engineering, vol. 63, no. 1, pp. 47–61 (2014).
- [13] Li W., Zhang X., Cheng S., Cao J., *Thermal Optimization for a HSPMG Used for Distributed Generation Systems*, IEEE Transactions on Industrial Electronics, vol. 60, no. 2, pp. 474–482 (2013).
- [14] Wu Q., Xiong H., Liu L., Meng G., Li H., Zhou L., *Research on voltage regulation of a permanent magnet generator*, 2011 International Conference on Electrical and Control Engineering, Yichang, China, pp. 4935–4937 (2011).
- [15] Qazalbash A., Sharkh S.M., Irenji N.T., Wills R.G., Abusara M.A., *Rotor eddy loss in high-speed permanent magnet synchronous generators*, IET Electric Power Applications, vol. 9, no. 5, pp. 370–376 (2015).